IEEE/CSC & ESAS European Superconductivity News Forum (ESNF), No. 15, January 2011
The published version of this manuscript appeared in *IEEE Transactions on Applied Superconductivity* **21**, Issue 3, 3166 - 3170 (2011)

# Composition Effects on the Critical Current of MOCVD-processed Zr:GdYBCO Coated Conductors in an Applied Magnetic Field

Yimin Chen[1], Tuo Shi[2], Albert P. Guevara[2], Yangxin Zhang[2], Yao Yao[2], Ibrahim Kesgin[2], and Venkat Selvamanickam[2]

***Abstract*— Zr:GdYBCO films were grown by reel-to-reel metal organic chemical vapor deposition (MOCVD) on hastelloy tapes with IBAD-MgO-based buffer. The composition was varied systematically to investigate the effects of changes in (Gd+Y)/Ba, (Gd+Y)/Cu and Gd/Y ratios and Zr-doping concentration on the critical current density ($J_c$) of the films in an applied magnetic field (B). The magnetic-field-angle dependence of $J_c$ measured at 77K and 1T showed that (1) for Gd+Y content ranging from 1.2 to 1.5, the minimum $J_c$ for any angle did not vary significantly with the Gd+Y content; while the $J_c$ at B//c varied significantly and took its maximum value at Gd+Y content of 1.2; (2) increasing Gd+Y could suppress or level off the $J_c$ peak at B//c which was associated with the pinning from $BaZrO_3$ nano-columns; (3) the optimum Zr-concentration for the highest $J_c$(77K, 1T) is in the range of 0.04 – 0.07 in the film; in this range under certain growth condition, the c-peak in the angular dependence of $J_c$ could be higher than the ab-peak; (4) increasing Gd/Y ratio increased $J_{c\_min}$(77K, 1T); (5) in self-field or low field, however, the optimized Gd/Y ratio was about 1.**

***Index Terms* — Composition effects, MOCVD, YBCO, 2G HTS, Coated conductor**

## I. Introduction

The study of composition effect on the superconducting properties of YBCO films began soon after the discovery of YBCO [1]-[3] and there have been many publications on this subject. Most of the publications were on optimizing the ratios of Y/Ba and Y/Cu for highest self-field critical current density.

The earliest study on the structure and distribution of excess yttrium in YBCO thin films and their effects on the magnetic field dependence of critical current density $J_c$ was the work by Lu et al. [2]. They showed that $Y_2O_3$ precipitates were effective flux pinning centers. Wang et al. [4] reported that the optimum Y content for highest $J_c$ was 1.1. Chen and Selvamanickam indicated [5]-[7] that $RE_2O_3$ (where RE = rare earth) nano-sized particles could form lines or layers parallel to the ab-plane and thus enhance the flux pinning in the ab-plane.

Manuscript received 3 Aug 2010. This work was supported in part by the U.S. Department of Energy through a contract with UT-Battelle.

Y. Chen is with SuperPower Inc, Schenectady, NY 12304 USA. E-mail: ychen@superpower-inc.com.

T. Shi, A. P. Guevara, Y. Zhang, Y. Yao, I. Kesgin and V. Selvamanickam are with Department of Mechanical Engineering and Texas Center for Superconductivity, University of Houston, Houston, TX 77204 USA.

The first significant progress towards creating effective extrinsic pinning defects was the study by Driscoll et al. [8], in which randomly oriented $BaZrO_3$ (BZO) particles of size 5-100 nm were incorporated within YBCO films grown by pulsed laser deposition (PLD). Subsequently, a report by Goyal et al. [9] showed that columnar defects of size 5-10nm, comprised of nanodots of BZO, aligned along the c-axis of YBCO can be incorporated within YBCO films made via PLD. Chen and Selvamanickam et al. [5], [6], [10] reported strong enhancement of flux pinning in Zr:GdYBCO coated superconducting tapes made via reel-to-reel metal organic chemical vapor deposition (MOCVD). We explained the enhancement and suppression of ab-peak and c-peak through the model of bi-dimensional pinning defects [5]. We indicated that the Zr-defects in REBCO films made via MOCVD could be effective pinning centers only for appropriate film compositions specified by RE/Ba and RE/Cu.

Substitutions of lanthanides for Y or mixtures of two or three lanthanides in REBCO could also introduce some effective pinning centers [10]-[13]. Takahashi et al [13] reported that $GdBa_2Cu_3O_{7-x}$ (GdBCO) coated conductor showed in-magneticfield performance superior to YBCO. They achieved $I_c$ of 522A/cm for short sample of 3.6μm thick GdBCO film on PLD-$CeO_2$ capped IBAD-$Gd_2Zr_2O_7$ buffered hastelloy metal substrate in self field at 77K [14]. Chen and Selvamanikam et al. [5], [10] reported that GdYBCO films with half Gd and half Y showed self-field $J_c$ superior to GdBCO or YBCO. We achieved $I_c$ of 813A/cm-width for meter-long tape of 3.3μm thick ZrGdYBCO film on hastelloy substrate with IBAD-MgO-based butter.

In order to improve the properties of second generation high temperature superconductor (2G HTS), it is crucial to improve the understanding on how the composition ratios RE/Ba and RE/Cu influence the shape, distribution and pinning properties of the extrinsic defects in REBCO films. However, systematical study on the composition effects for REBCO film with extrinsic defects created via highly doping has not been reported.

In this paper, we study the effects of composition on the magnetic field dependences of $J_c$ for Zr:GdYBCO coated superconducting tapes through systematically varying the ratios of (Gd+Y)/Ba, (Gd+Y)/Cu and Gd/Y and the Zr-concentration.

## II. Experimental Details

SuperPower prototype reel-to-reel MOCVD apparatus was used to deposit the Zr:GdYBCO films. The liquid-source precursor delivery unit in this MOCVD system is equipped with a SuperPower proprietary injector which enables the stability of delivery of the heavy metal precursor. The single liquid source was made by mixing the organometallic tetramethyl heptanedionate (thd) compounds for Zr, Gd, Y, Ba and Cu in tetrahydrofuran solution at appropriate mole ratio. The solution delivery rate was controlled by a fluid metering pump. The precursor solution was vaporized in the evaporator and the chemical vapor generated in the evaporator was carried by argon gas to the MOCVD reactor. The vertical flow of carrier gas and organometallic vapor in the reactor is distributed by a close-coupled showerhead and a vapor guide. Many short sample tapes at a variety of MOCVD conditions can be processed in a single run. This is important for the reliability of the experimental results because carrying out many experiments in single run can ensure the experiments to be all conducted under the same hardware configuration.

In all MOCVD processes for Zr:GdYBCO films in the present work, the chamber pressure was 2.3 Torr, the oxygen partial pressure was 0.9 Torr, the deposition rate was controlled at about 0.2 μm/min, except explicitly specified. The deposition temperature was optimized for every precursor composition.

The fabrication details of the buffered substrate architecture, Hastelloy-substrate\$Al_2O_3$\$Y_2O_3$\IBAD-MgO\MgO\$LaMnO_3$, was described in our previous publications [6]. The in-plane texture of the cap layer, $LaMnO_3$ (LMO), of the buffer stack for the tapes used in present work was 7.7° full-width-at-half maximum (FWHM) as measured by X-ray Diffraction (XRD) phi-scans about LMO (110).

The compositions of the Zr:GdYBCO films were measured by inductively coupled plasma atomic emission spectroscopy (ICP-AES). To study the microstructure in the films, X-ray diffraction (XRD) analysis including $\theta$–$2\theta$ scan and $\phi$ scan and transmission electron microscope (TEM) were performed.

## III. Results and Discussions

### A. Composition Control in MOCVD for Zr:GdYBCO

The film/precursor composition ratio for an element in MOCVD is defined as the ratio of the relative mole concentration of the element in the film to that in the precursor. It varies with the MOCVD conditions such as temperatures and pressure. In order to control the composition in MOCVD, the film/precursor composition ratio for each of the elements needs to be established as a function of process parameters.

Fig. 1 shows the film/precursor composition ratios for Zr, Gd, Y, Ba and Cu as a function of the susceptor temperature at a pressure of 2.3 Torr. Fig. 2 shows the pressure dependences of the film/precursor composition ratios at the susceptor temperature of 970°C. The film composition control was related to the precursor composition through these functions.

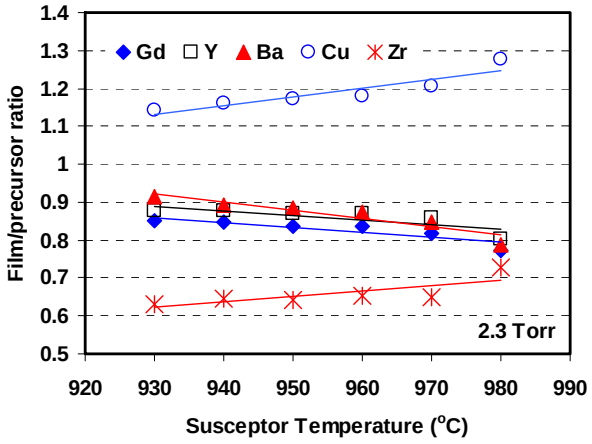


Fig. 1. Ratio of film composition to precursor composition as a function of susceptor temperature for Gd, Y, Ba, Cu and Zr in MOCVD for Zr:GdYBCO.

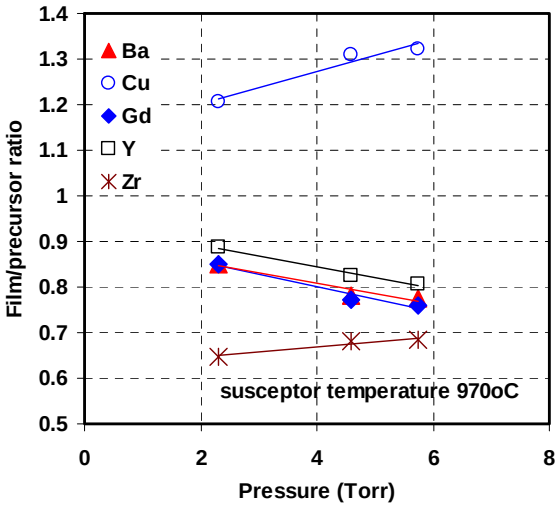


Fig. 2. Ratio of film composition to precursor composition as a function of chamber pressure for Gd, Y, Ba, Cu and Zr in MOCVD for Zr:GdYBCO.

### B. Effects of Gd+Y content in GdYBCO

In MOCVD for REBCO films, the film composition should be off from the 123 stoichiometry to achieve high critical current ($I_c$) [5]. It was found that in RE rich films, the Ba-Cu-O phases were minimized. Furthermore, the excess amount of RE results in precipitates of $RE_2O_3$ which are effective pining centers to increase the $I_c$.

In our analysis with XRD, SEM and TEM, we did not observe RE-211 phase in the RE rich films; instead, a high density of $(Y,Gd)_2O_3$ nano-precipitates was found in the Zr:GdYBCO films with an average size of ~9nm as determined via X-ray diffraction peak-broadening analysis. The $RE_2O_3$ nano-particles were highly oriented with respect to the RE-123 matrix. Some of them were aligned in lines in the *ab* plane of the GdYBCO film.

Fig. 3 shows magnetic-field-angle dependences of the $J_c$ for GdYBCO films with various Gd+Y contents. Film compositions of Ba=2 and Cu=3.3 are fixed for all samples in Fig. 3. The film thicknesses are all about 0.5μm. The $J_c$ is improved with increasing RE from 1 to 1.2. For Gd+Y = 1.3, 1.4 and 1.5, the $J_c$ shows strong peak at B//*ab* (270°).

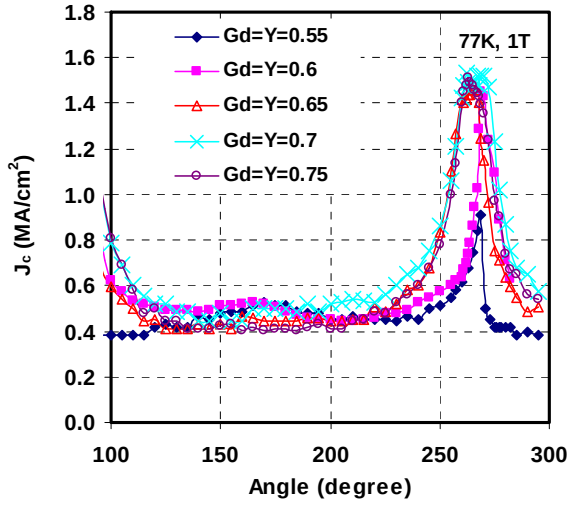


Fig. 3. Critical current density as a function of angle between magnetic field and normal to the film surface of GdYBCO on IBAD substrate with film composition of Ba=2, Cu=3.3, and Gd & Y values labeled on the curves.

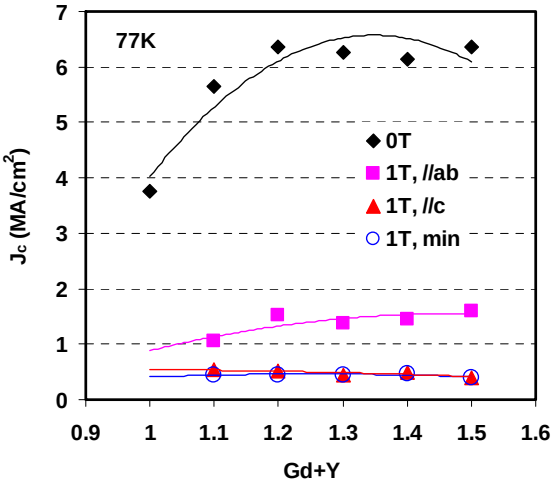


Fig. 4. RE-content dependence of $J_c$ for GdYBCO at (1) self-field (0T); (2) B=1T & **B**//ab; (3) B=1T & **B**//c; (4) minimum $J_c$ for any angle at B=1T. For all the RE-content, Ba=2, Cu=3.3, and Gd=Y.

The RE-content dependences of self-field $J_c$ ($J_c$(sf)), $J_c$(B=1T, **B**//ab), $J_c$(B=1T, **B**//c) and $J_{c\ min}$(B=1T,any angle) for GdYBCO are given in Fig. 4. The sample with RE content 1.2 shows the highest $J_c$ for both in self field and in applied magnetic field. Further increasing Gd+Y in GdYBCO films up to RE=1.5 did not significantly reduce $J_c$(sf) or $J_c$(B). This finding is in contrast to that reported for YBCO films fabricated by PLD [4] where Y contents above the optimum value (1.1) results in reduction of $J_c$(sf) and $J_c$(B) dramatically.

### *C. Effects of Gd+Y content in Zr:GdYBCO*

In the case of GdYBCO without extrinsic doping, the $J_c$ peak at B//c was not influenced much by varying the Gd+Y content. The situation changed when Zr was added.

Fig. 5 displays the RE-content dependences of of $J_c$(sf), $J_c$(B=1T, **B**//ab), $J_c$(B=1T, **B**//c) and $J_{c\ min}$(B=1T,any angle) for 0.5μm-thick Zr:GdYBCO grown on IBAD substrate. As seen from the figure, the in-field performance changes significantly with varying RE content. The minimum $J_c$ for any field direction is maximum at around Gd+Y=1.3. $J_c$(1T, **B**//c) is maximum at around Gd+Y content of 1.2, while Gd+Y=1.5 gives the strongest $J_c$ peak at B//ab.

Fig. 6 shows angular dependence of $J_c$ for ZrGdYBCO films with Gd+Y contents of 1.1, 1.2 and 1.5 in 1T magnetic field and 77K temperature. Note that the $J_c$ peak at **B**//ab is leveled off for Gd+Y content less than 1.1. On the other hand, when Gd+Y increases to 1.5, the $J_c$ peak at **B**//c is leveled off while the ab-peak is strongly enhanced. For Gd+Y=1.2, however, both c-peak and ab-peak exist and they are quite broad.

It is interesting that the minimum of $J_c$(B=1T) for ZrGdYBCO samples with Gd+Y=1.5 remains as high as about double of the magnitude as that for GdYBCO films without Zr addition, though the c-peak is leveled off.

For Gd+Y=1.2, the microstructure is characterized with bidirectionally aligned defects embedded in perfect GdYBCO crystalline matrix. The BZO columnar defects are well formed, which is responsible for the strong pinning for B//c.

For Gd+Y=1.5, the microstructure is dominated by layers of $RE_2O_3$ nano-precipitates, which is responsible for the strong enhancement of pinning in ab-plane. The BZO columns have been broken into many pieces, which could explain the suppression of c-peak.

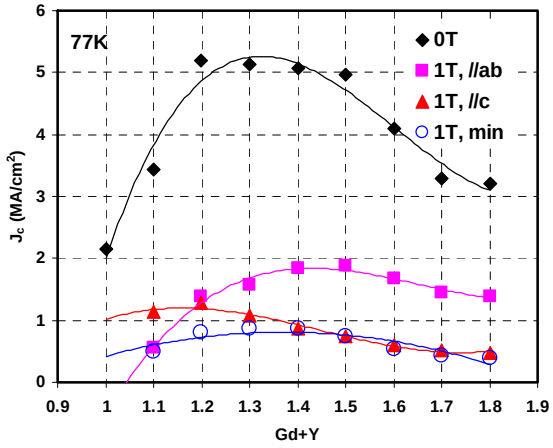


Fig. 5. RE-content dependence of $J_c$ for ZrGdYBCO at (1) self-field (0T); (2) B=1T & **B**//ab; (3) B=1T & **B**//c; (4) minimum $J_c$ for any angle at B=1T. The compositions for all the ZrGdYBCO films are of Ba=2, Cu=3.3, Zr=0.055 and Gd=Y. The film thicknesses are about 0.5μm.

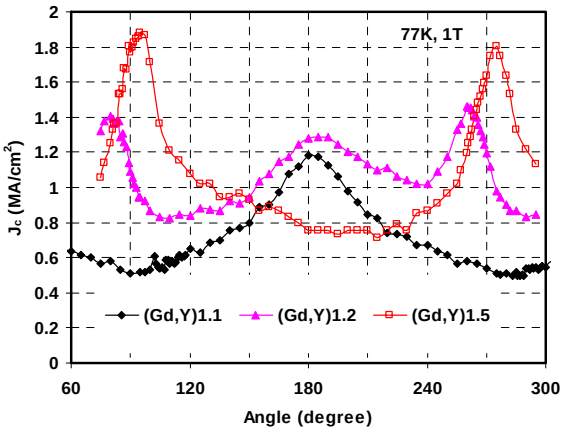


Fig. 6. Magnetic-field-angle dependence of $J_c$ for ZrGdYBCO films with RE content (Gd+Y) of 1.1, 1.2, and 1.5. The compositions are of Ba=2, Cu=3.3, Zr=0.055 and Gd=Y. The film thicknesses are about 0.5μm.

### D. *Effects of Gd/Y in Zr: GdYBCO*

Displayed in Fig. 7 are Gd/Y-ratio dependences of $J_c$(sf), $J_c$(1T, //ab), $J_c$(1T, //c) and $J_{c\ min}$(1T, any angle) for 0.5μm-thick ZrGdYBCO films. For all the ZrGdYBCO films, Ba=2, Cu=3.3, Zr=0.055 and Gd+Y=1.2. The film thicknesses are about 0.5μm. As seen from the figure, self-field $J_c$ takes maximum at Gd/Y=1. The $J_c$(1T, 77K), however, is improved with increasing Gd/Y. Fig. 8 shows the angular dependence of the critical current density for $Zr_{0.055}Y_{1.2}Ba_2Cu_{3.3}O_7$, $Zr_{0.055}Gd_{1.2}Ba_2Cu_{3.3}O_7$ and $Zr_{0.055}Y_{0.6}Gd_{0.6}Ba_2Cu_{3.3}O_7$. GdBCO showed higher $J_c$(77K, 1T) for any angle.

When measured at a lower temperature of 65K, however, YBCO showed better performance than GdBCO. The properties for the films at low temperature and high field will be reported in a separated paper.

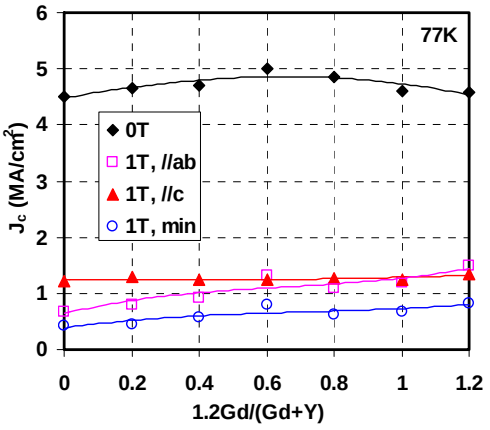


Fig. 7. Gd-to-Y ratio dependences of $J_c$(0T), Jc(1T, //ab), Jc(1T, //c) and $J_{c\_min}$(1T, any angle) for ZrGdYBCO films with Ba=2, Cu=3.2, Zr=0.055 and Gd+Y=1.2.

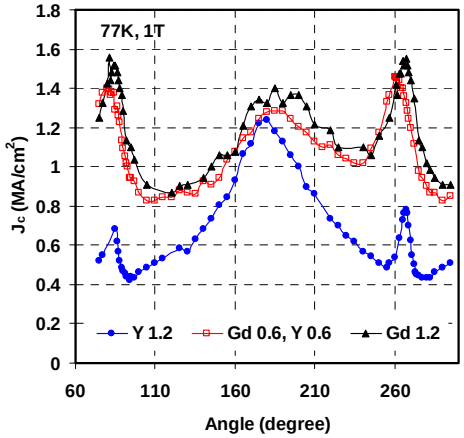


Fig. 8. Magnetic-field-angle dependence of $J_c$ for $Zr_{0.055}Y_{1.2}Ba_2Cu_{3.3}O_7$, $Zr_{0.055}Gd_{1.2}Ba_2Cu_{3.3}O_7$ and $Zr_{0.055}Y_{0.6}Gd_{0.6}Ba_2Cu_{3.3}O_7$. The film thicknesses are about 0.5μm.

### E. *Effects of Zr concentration*

Fig. 9 shows the Zr-concentration dependence of critical current density $J_c$ for $Y_{0.6}Gd_{0.6}Ba_2Cu_{3.3}O_7$ doped with Zr. Seen from the figure, $J_c$(1T, //c) , or c-peak, varies significantly with Zr-concentration. For Zr-concentration in the range of 0.04 – 0.075, c-peak can be higher than or the same height as ab-peak. $J_{c\_min}$(1T, any angle) also takes its optimum value, ~ 0.8MA/cm$^2$, for Zr-concentration in this range, which is double the value for GdYBCO without Zr doping.

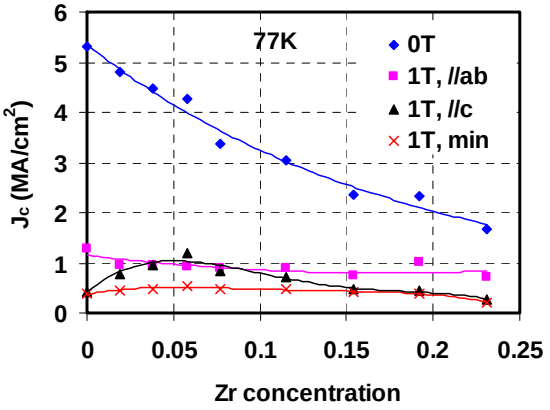


Fig. 9. Zr-concentration dependence of $J_c$ for $Zr_x$:$Gd_{0.6}Y_{0.6}Ba_2Cu_{3.3}O_7$ at (1) self-field (0T); (2) B=1T & **B**//ab; (3) B=1T & **B**//c; (4) minimum $J_c$ for any angle at B=1T. The film thicknesses are about 0.5μm.

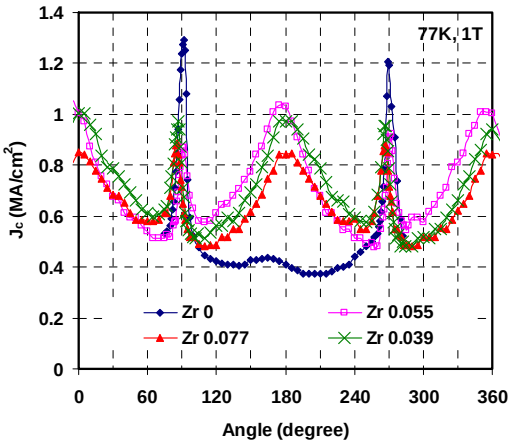


Fig. 10. Angular dependence of $J_c$ for Zr doped $Gd_{0.6}Y_{0.6}Ba_2Cu_{3.2}O_7$. The film thicknesses are about 0.5μm.

Pinning is optimized when the size of the defects approaches the superconducting coherence length (about 2 nm for YBCO at 77K) and when the area number density of defects is the order of B×10$^{11}$ cm$^{-2}$ [15], [16]. The $J_c$(1T, //c) curve in Fig. 9 shows that Zr-concentration ranging from 0.04 to 0.075 is a necessary condition for optimum pinning effect along c-axis. At certain growth condition, the BZO nanocolumns are well aligned in the c-direction and the area number density of the nanocolumns is appropriate to form correlated pinning centers. The correlated pinning centers will strongly enhance the c-peak in the angular dependence of $J_c$ for intermediate magnetic field ranging from 0.4T to 2T. Simultaneously, the well-formed columnar defects penetrating through the film will break the horizontal layers comprised of $RE_2O_3$ nanoprecipitates and suppress the ab-peak. It thus results in the c-peak stronger than ab-peak for magnetic field in the range of 0.4T-2T. Therefore, the happen of c-peak being stronger than ab-peak depends on the growth condition and film composition as well as the Zr-concentration.

Fig. 10 displays the angular dependence of $J_c$ at 77K and 1T for various Zr concentrations. For Zr-concentrations of 0.039, 0.055 and 0.077, the infield performance is improved significantly over the undoped sample. The tapes with Zr-concentration of 0.055 are of the best performance in 1T and 77K.

## ACKNOWLEDGMENT

We thank Dr. D. Miller of Argon National Laboratory for TEM analysis and Ms. S. Repnaya of SuperPower Inc. for ICP-AES analysis.

## REFERENCES

[1] J. Zhao, C. S. Chern, Y. Q. Li, P. Norris, B. Gallois, B. Kear, X. D. Wu, and R. E. Muenchausen, "Compositional effects on plasma-enhanced metalorganic chemical vapor deposition of $YBa_2Cu_30_{7-x}$ thin films", Appl. Phys. Lett. 58, 2839 (1991).

[2] P. Lu, Y. Q. Li, J. Zhao, C. S. Chern, B. Gallois, P. Norris, B. Kear, and F. Cosandey, "High density, ultrafine precipitates in $YBa_2Cu_3O_{7-x}$ thin films prepared by plasma-enhanced metalorganic chemical vapor deposition", *Appl. Phys. Lett*. vol. 60, pp.1265-1267, Jan. 1992.

[3] Y. Q. Li, J. Zhao, C. S. Chern, P. Lu, T. R. Chien, B. Gallois, P. Norris, B. Kear, F. Cosandey, "Effects of $Y_2O_3$ precipitates on critical current anisotropy in $YBa_2Cu_3O_{7-x}$ thin films prepared by plasma-enhanced metalorganic vapor deposition", Appl. Phys. Lett. vol. 60, pp. 2430, 1992.

[4] H. Wang, A. Serquis, B. Maiorov, L. Civale, Q. X. Jia, P. N. Arendt, and S. R. Foltyn, J. L. MacManus-Driscoll, X. Zhang, "Microstructure and transport properties of Y-rich $YBa_2Cu_3O_{7-x}$ thin films", *J. Appl. Phys*., vol. 100, 053904, 2006.

[5] Y. Chen, V. Selvamanickam, Y, Zhang, Y. Zuev, C. Cantoni, E. Specht, M.P. Paranthaman, T, Aytug, A. Goyal, D. Lee, "Enhanced flux pinning by $BaZrO_3$ and $(Gd,Y)_2O_3$ nano-structures in metal organic chemical vapor deposited GdYBCO high temperature superconductor tapes", *Appl. Phys. Lett*. vol. 94, 062513, Feb. 2009.

[6] V. Selvamanikam, Y. Chen, X. Xiong, Y. Xie, M. Martchevski, A. Rar, Y. Qiao, R. M. Schmidt, A. Knoll, K. P. Lenseth, and C. S. Weber, "High Performance 2G Wires: From R&D to Pilot-Scale Manufacturing", *IEEE Trans. Appl. Superconductivity*, vol. 19, no. 3, pp 3225-3239, June 2009

[7] T.G. Holesinger, B. Maiorov, O. Ugurlu, L. Civale, Y. Chen, X. Xiong, Y. Xie and V. Selvamanickam: Microstructural and superconducting properties of high current metal–organic chemical vapor deposition $YBa_2Cu_3O_{7-\delta}$ coated conductor wires, Supercond. Sci. Technol. **22,** 045025 (2009).

[8] J. L. Macmanus-Driscoll, S. R. Foltyn, Q. X. Jia, H. Wang, A. Serquis, L. Civale, B. Maiorov, M. E. Hawley, M. P. Maley and D. E. Peterson, "Strongly enhanced current densities in superconducting coated conductors of YBa2Cu3O7-x+$BaZrO_3$", Nature Materials **3**, 439 (2004).

[9] A. Goyal et al., "Irradiation-free, columnar defects comprised of self-assembled nanodots and nanorods resulting in strongly enhanced flux-pinning in $YBa_2Cu_3O_{7-\delta}$ films", *Supercond. Sci. Technol.* vol. 18, pp. 1533, Nov 2005.

[10] Y. Chen, X. Xiong, Y. Xie, Y. Qiao, X. Zhang, A. Rar, M. Martchevskii, R. Schmidt, K. Lenseth, J. Herrin, D. Hazelton, V. Selvamanickam, "Recent progress in second-generation HTS wire technology at SuperPower", MRS Online Proceedings, 2008 Spring Meeting, 1099-II01-02, Mar 2008.

[11] Y. Yoshida, Y. Ichino, M. Miura, Y. Takai, K. Matsumoto, A. Ichinose, S. Horii, M. Mukaida, "High critical current density in high field in $Sm_{1+x}Ba_{2-x}Cu_3O_{6+y}$ thin films", IEEE Transactions on Applied Superconductivity vol.15, pp. 2727, 2005.

[12] S. H. Wee, A. Goyal, Y. L. Zuev and C. Cantoni, "High performance superconducting wire in high applied magnetic fields via nanoscale defect engineering", Supercond. Sci. Technol., vol. 21, 092001, Sep 2008.

[13] K. Takahashi, Y. Yamada, M. Konishi, T. Watanabe, A. Ibi, T. Muroga, S. Miyata, Y. Shiohara, T. Kato and T Hirayama, "Magnetic field dependence of $J_c$ for Gd-123 coated conductor on PLD-$CeO_2$ capped IBAD-GZO substrate tapes", Supercond. Sci. Technol. vol. 18, pp. 1118, 2005.

[14] K. Takahashi, H. Kobayashi, Y. Yamada1, A. Ibi, H. Fukushima, M. Konishi, S. Miyata, Y Shiohara, T. Kato and T. Hirayama, "Investigation of thick PLD-GdBCO and $ZrO_2$ doped GdBCO coated conductors with high critical current on PLD-$CeO_2$ capped IBAD-GZO substrate tapes", *Supercond. Sci. Technol*. vol. 19, pp. 924, 2006.

[15] T. Matsushita, "Flux pinning in superconducting 123 materials" *Supercond. Sci. Technol*. Vol. 13, pp. 730-737, June 2000.

[16] David Larbalestier, Alex Gurevich, D. Matthew Feldmann & Anatoly Polyanskii, " High-$T_c$ superconducting material for electric power applications", Nature, vol. 414, pp. 368-377, Nov. 2001.